Front. Optoelectron. 2013, 6(2): 175–179
DOI 10.1007/s12200-013-0311-4

RESEARCH ARTICLE

Reflected-intensity distribution of angle-tuned thin film filter based on frequency recursive algorithm

Kan YU (✉), Juanjuan YIN, Jiaqi BAO

Huazhong University of Science and Technology Wenhua College, Wuhan 430074, China

Abstract For a three-port angle-tuned thin film filter, the characteristic of reflected-port is very important to reflect multiple wavelengths spectrum. As the filter is in tilted incidence, the reflected-facula broadens and the reflectivity decreases. In this paper, we proposed a frequency recursive algorithm based on fast Fourier transform and Fresnel formula. The reflected-intensity distribution of the narrowband filter from normal incidence to 40° tilted incidence was simulated by this frequency recursive algorithm. Meanwhile, the beam field experiments were accordingly performed in this study. Compared with the traditional beam spatial superposition method, the frequency recursive algorithm is more efficient and precise in calculating the reflectivity of the reflected beam, suggesting the frequency recursive algorithm may be more helpful for fabricating the three-port tunable thin film filter.

Keywords thin film filter, recursive algorithm, tilted incidence, fast Fourier transform

1 Introduction

With low insert loss, good temperature stability and narrowband, thin film interference filter in dense wavelength division multiplexing (DWDM) system is widely used [1,2]. Traditional narrowband thin film filter only can be used in normal incidence due to its serious polarization sensitivity [3]. With the development of the technology of polarization insensitivity, more and more attentions have been paid to angle-tuned thin film filter for its simple structure and low cost [4,5]. In the DWDM system, a three-port tunable filter can be used to select the specific wavelength out of multiple wavelengths, and the residual wavelengths will be transmitted in the fiber without any disruption [6]. So the reflectivity and the bandwidth in tilted incidence are the key characteristics of the reflected port. In our previous research, the reflected-intensity distribution of the filter has been derived based on the multi-beam interference principle and Gaussion beam transmission equation [7]. However, the simulation results obtained by the beam spatial superposition method have high error relative to the corresponding experimental results for its reflectivity [8]. So we proposed a frequency recursive algorithm in this study to research the reflected beam characteristics of the thin film filter used in tilted incidence. The reflectivity and the reflected-facular broadening were deduced with different incident angle, and according experiments were performed to test the simulation results.

Received January 6, 2013; accepted February 22, 2013

E-mail: onlyfish@126.com

2 Theoretical analysis

The thin film filter with multiple cavities and narrowband has a simple structure with the high refractive index, in which low refractive index materials is placed at regular intervals as well, and they are both quarter wavelength coatings [9]. Usually the incident beam of the thin film filter is Gaussian beam, which can be considered as a plane wave at its waist radius. Each point in the reflection light field has the same reflected characteristic when the thin film filter is in normal incidence. While the incident angle increase reflected characteristic will be different due to the relative displacement of the reflected beam,

The reflected Gaussian beam field distribution is demonstrated in Fig. 1. It shows a single layer film with the thickness d_1 and refractive index n_1, and this singer layer film has two interfaces M_1 and M_2. The incident and reflected medium is air with the refractive index n_0. When an incident Gaussian beam E_0 on the film with an angle of θ_0 (the refraction angle in the layer is θ_1), the light field of the first reflected beam is E_1. The subsequent reflected multiple light fields are E_2, E_3,..., E_m. The total reflected

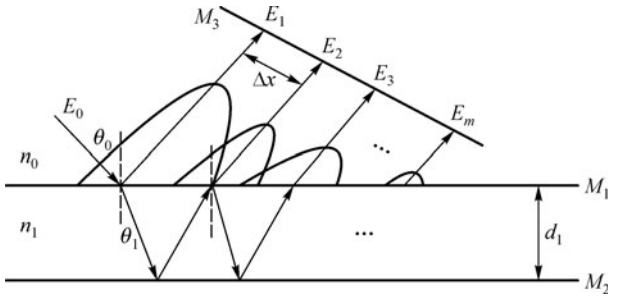

Fig. 1 Reflected-intensity distribution in single layer film in tilted incidence

light intensity E_t can be described as $E_t = \sum_{k=1}^{m} E_k$ on the measured surface M_3.

The incident beam can be written as [10,11]

$$E(x,y) = A_0 \exp\left[-\frac{x^2+y^2}{\omega_0^2}\right], \tag{1}$$

where ω_0 is the beam waist, A_0 is the field amplitude of the incident beam waist center, x and y represent the coordinates of the incident beam field horizontal distribution. If the r and t are the reflection and transmission coefficients of the coating, the reflected beam fields are plain sequence as

$$E_1 = rE_0,$$

$$E_2 = t^2 r E_0 \mathrm{e}^{\mathrm{j}\delta},$$

$$E_3 = t^2 r^3 E_0 \mathrm{e}^{2\mathrm{j}\delta},$$

$$\cdots$$

Using the Fresnel formula, the total reflected beam field can be derived as

$$E_k = \sum_{k=1}^{n} t^2 (r)^{2k-1} E_0[x-(k-1)] \cdot \Delta x_1 \cdot \exp[-\mathrm{j}(k-1)\delta_1], \tag{2}$$

where $\delta = \frac{2\pi}{\lambda} n_1 d_1 \cos\theta_1$ is the single reflection phase shift of the beam, and Δx_1 is the relative displacement of the adjacent beams, and it can be described as

$$\Delta x_1 = 2n_1 d_1 \sin\theta_1. \tag{3}$$

3 Algorithm design

We have fabricated an angle-tuned thin-film filter with four cavities used in 100 GHz DWDM channel spacing according to stack (4) in the Filtech Corporation in China.

$$\begin{bmatrix} (HL)^7 2L3H4L3H2L(LH)^7 L(HL)^8 2L3H4L3H2L(LH)^8 L \\ (HL)^8 2L3H4L3H2L(LH)^8 L(HL)^7 2L3H4L3H2L(LH)^7 \end{bmatrix} \tag{4}$$

In the stack (4), the high refractive index material H is Ta_2O_5 ($n = 2.06$) and the low refractive index material L is SiO_2 ($n = 1.465$), which are both quarter wavelength coatings. So the thickness of the high and low refractive index material can be described as Eq. (5).

$$d_H = \lambda_0/(4n_H),\ d_L = \lambda_0/(4n_L). \tag{5}$$

The central wavelength is 1563 nm when the angle-tuned thin film filter is in the normal incidence. It has a stable angle-tuned transmission characteristics and it also eliminate the central wavelength separation phenomena of the two polarization modes by optimizing the spacer. The incident angle range of the angle-tuned thin film filter is from 0° to 15°, so that its tunable central wavelength can cover the range from 1563 to 1545 nm. This stack use both high and low index materials as the spacer to eliminate the polarization light central wavelength separation, so it has low polarization-sensitivity within tunable range.

Based on the fast Fourier transform, we proposed a frequency recursive algorithm. The implementation process of the algorithm is described as follows:

1) Get the beam field sequence $\{E_0(x_N)\}$ by sampling the incident beam field E_0 in the x-axis, then get the $\{E_0(u_N)\}$ from the $\{E_0(x_N)\}$ by the fast Fourier transform, where the sample number is $N+1$,

$$x_N = \{0,1,2,...,N\} \cdot dx$$

and

$$u_N = \frac{\{0,1,2,...,N\}}{N \cdot dx};$$

2) Calculate the included angle

$$\theta_i = \arcsin(n_0 \sin\theta_0 / n_i)$$

to the normal line in the coating i (i = 1, 2, 3,…, $m+1$);

3) Get the he reflection r_i coefficient and the and transmission coefficient t_i of coating i according to the Fresnel formula;

4) Calculate the reflection phase shift

$$\delta_i = \frac{2\pi}{\lambda} n_i d_i \cos\theta_i$$

in the coating i;

5) Calculate the relative displacement

$$\Delta x_i = 2n_i d_i \sin\theta_i$$

of the adjacent beams;

6) Calculate the phase factor

$$p_i = \exp\left(-\mathrm{j}(\delta_i + 2\pi \cdot \Delta x_i \cdot u_N)\right)$$

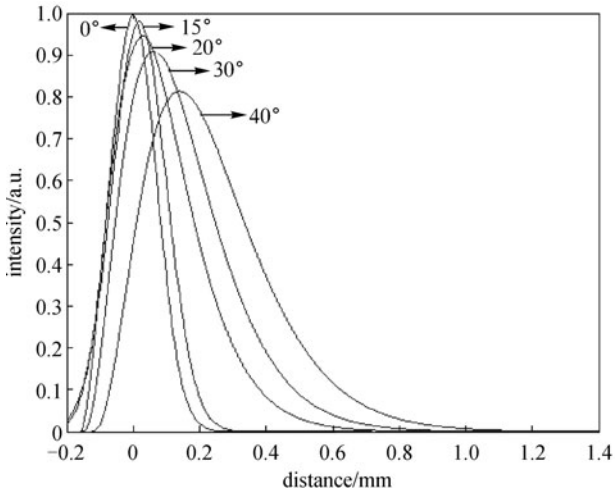

Fig. 2 Reflected-intensity distribution with different incident angles on filter

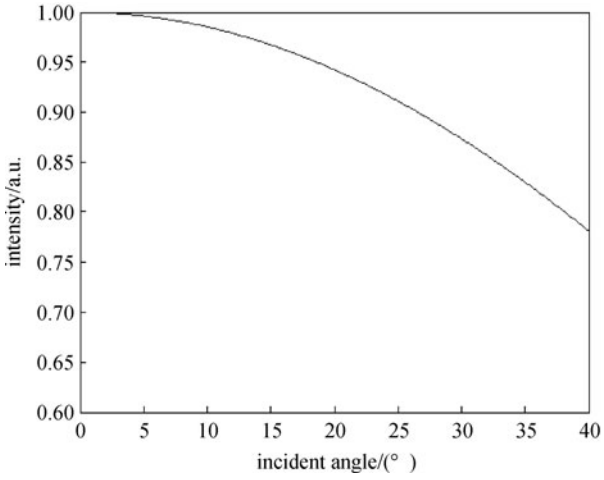

Fig. 3 Reflectivity with different incident angles on filter

of each coating in the frequency domain;

7) Get the reflected beam field sequence $\{E_t(u_N)\}$ according to the phase factor based on the fast Fourier transform;

8) Get the final reflected beam field distribution of the whole stack by the fast Fourier inverse transform.

As can be seen from the above description of the algorithm, we calculated the reflected-intensity distribution of the angle-tuned thin film filter with different incident angles.

In Fig. 2, the energy profile of the total reflected beam intensity distribution is shown for $\omega_0 = 0.23$ mm with different incident angle (0°, 15°, 20°, 30° and 40°). From Fig. 2, it can be seen that the reflectivity is 100% and the reflected-intensity has a Gaussian distribution in normal incidence. As the incident angle is increasing, the reflectivity is decreasing and the reflected-facular is broadening, and the reflected beam peak is shifting to the reverse direction of the incident angle.

Figure 3 shows the reflectivity with different incident angles. Figure 3 shows that the reflectivity decreases slowly and it still has the reflectivity of 80% in 40° tilted incidence. However, the traditional beam spatial superposition method only can be employed to simulate the reflected-facular broadening, and its reflectivity has been kept 100% with any incident angle. As the incident angle increases, the displacement of the adjacent beam will decrease. It will induce the reflectivity decreasing. Compared with the traditional beam spatial superposition method, the frequency recursive algorithm is more precise.

4 Experiments

The beam field experiments are performed by a Beam-Master system, which is an beam profilers using two orthogonal knife-edges or slits to scan the beam profile. Figures 4(a) and 4(b) show the measured reflected beam field distribution of the angle-tuned thin film filter at the incident angles of 0° and 15°, respectively.

As shown in Fig. 4, the reflected beam field is circular symmetric at normal incidence, and the center of the field has the maximum reflected peak. At 15° incidence, the reflected beam field broadens along vertical axis, and the reflected peak has a little vertical displacement, which cause the decreasing of the channel isolation degree. The dimension of beam field distribution with 15° incidence is approximately 1.2 times of that with normal incidence. The experimental results are coinciding with those of the theoretical simulation.

As a three-port tunable filter, the isolation degree of the reflected port is very important. In 100 GHz DWDM system, the reflected isolation degree should be more than 25 dB. Figure 5 shows the reflected multiple wavelengths spectrum of the angle-tuned thin film filter. From Fig. 5, the bandwidth of the reflected spectrum in 15° tilted incidence is larger than that in normal incidence, and the 15° tilted incidence isolation degree (28 dB) is much lower than that of the isolation degree (38 dB) in normal incidence.

5 Discussion

Figure 6 shows the reflected-intensity distribution of the thin film filter in 15° incidence based on the traditional beam spatial superposition method [8]. As shown in Fig. 6, the beam field distribution presented multiple reflected peaks and its dimension is more than 2 times of that with normal incidence, which is not coincide with the experimental results. The Beam-Master experiment system shows that the reflected beam field distribution of the filter

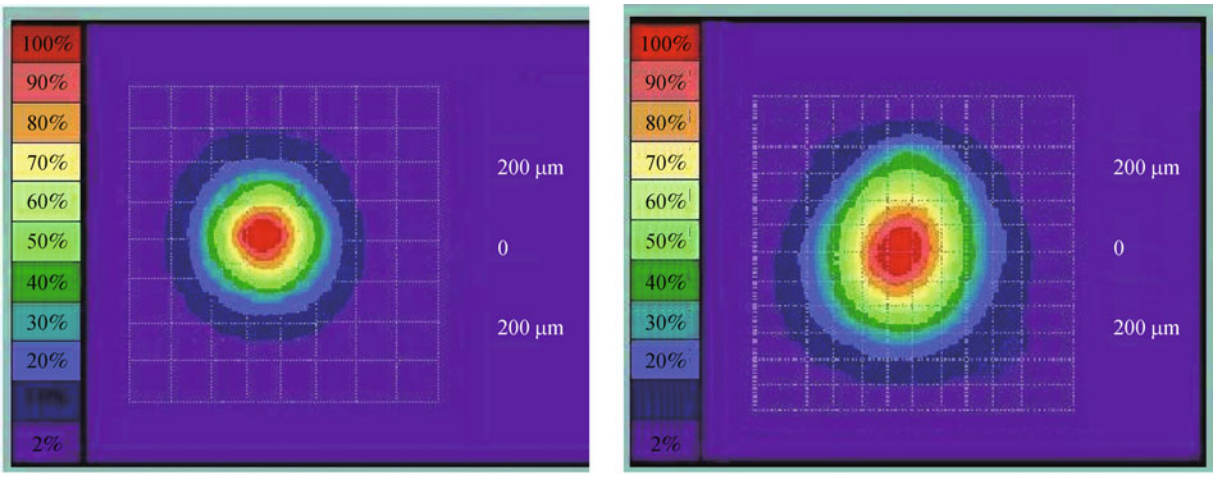

Fig. 4 Reflected-intensity distribution on the filter at the incident angles of (a) 0° and (b) 15°

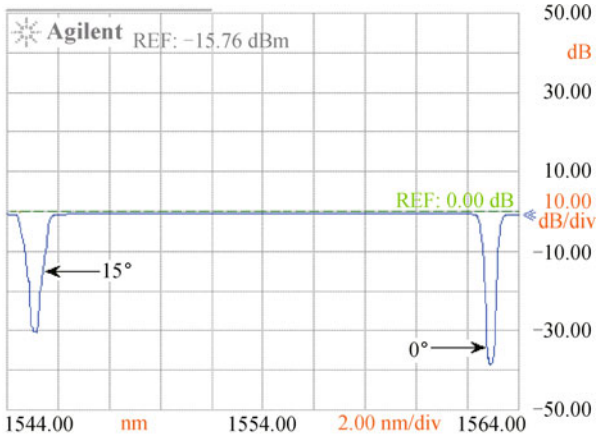

Fig. 5 Reflected spectrum on filter

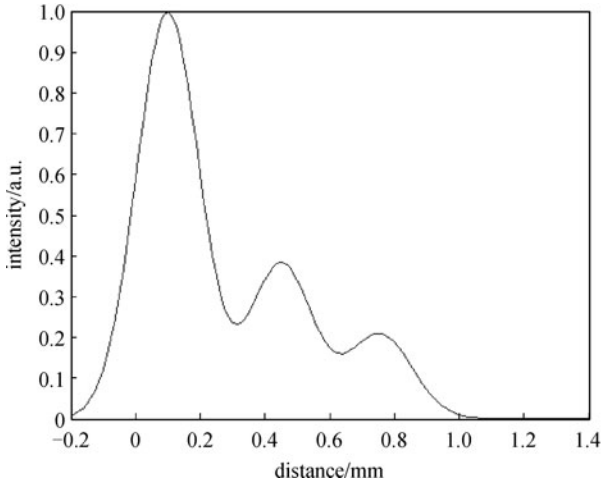

Fig. 6 Reflectivity with 15° incident angle on filter by beam spatial superposition method

at 15° tilted incidence has only one reflected peak, and its dimension is approximately 1.2 times of that with normal incidence. So the frequency recursive algorithm is more precise in calculating the reflected beam field distribution.

6 Conclusions

In summary, in this paper, a frequency recursive algorithm based on the fast Fourier transform was proposed, and the reflected-intensity distribution of the angle-tuned thin film filter in tilted incidence was calculated. The simulation results are coinciding with those of the experiments. Compared with the traditional beam spatial superposition method, the frequency recursive algorithm is more efficient and precise in calculating the reflectivity of the reflected beam. Consequently, the frequency recursive algorithm may be more helpful for fabricating the three-port tunable thin film filter.

Acknowledgements This work was supported by the National Natural Science Foundation of China (Grant No. 61205062) and the Nature Science Foundation of Hubei Province of China (No. 2012FFB02701).

References

1. Antonio-Lopez J E, Castillo-Guzman A, May-Arrioja D A, Selvas-Aguilar R, Likamwa P. Tunable multimode-interference bandpass fiber filter. Optics Letters, 2010, 35(3): 324–326
2. Xie J, Chen Y P, Lu W J. Tunable optical bandpass filter with multiple flat-top bands in nanostructured resonators. Optical Engineering, 2011, 50(3): 0340051–0340055
3. Tournois P. Design of acousto-optic programmable filters in mercury halides for mid-infrared laser pulse shaping. Optics Communications, 2008, 281(15–16): 4054–4056

4. Domash L, Wu M, Nemchuk N, Ma E. Tunable and switchable multiple-cavity thin film filters. Journal of Lightwave Technology, 2004, 22(1): 126–135
5. Hirokal T, Hirano T, Guan P. PMD-induced crosstalk in ultrahigh-speed polarization multiplexed optical transmission in the presence of pdl. Journal of Lightwave Technology, 2011, 29(19): 2966–2970
6. Yu K, Liu W, Huang D X, Chang J. C-band three-port tunable band-pass thin film optical filter with low polarization-sensitivity. Optics Communications, 2008, 281(14): 3709–3714
7. Zhou X, Lu C, Shun P. A performance analysis of an all-optical clock extraction circuit based on Fabry-Perot filter. Journal of Lightwave Technology, 2001, 19(5): 603–613
8. Yu K, Huang D X, Yin J J. Reflected-intensity distribution of a thin-film filter with oblique incidence of a Gaussian beam under-parallel case. Chinese Journal of Lasers, 2012, 39(8): 0807003(1–6)
9. Wang X Z, Zhu T, Chen L, Bao X. Tunable Fabry-Perot filter using hollow-core photonic bandgap fiber and micro-fiber for a narrow-linewidth laser. Optics Express, 2011, 19(10): 9617–9625
10. Wu Z M, Xia G Q, Zhou H Q, Wu J, Liu M. Transmission of a Gaussian beam after incidenting nonnormally on a Fabry-Perot etalon. Optics & Laser Technology, 2003, 35(1): 1–4
11. Liu M L, Chao X B, Ye Z Q. Transmitting intensity distribution after a Guassian beam incidenting nonnormally on a wedged Fabry-Perot cavity. Optik-International Journal for Light and Electron Optics, 2008, 119(14): 661–665